Journal of Power Sources 194 (2009) 536–540

Contents lists available at ScienceDirect

Journal of Power Sources

journal homepage: www.elsevier.com/locate/jpowsour

The defect chemistry of $LiFePO_4$ prepared by hydrothermal method at different pH values

Jiali Liu, Rongrong Jiang, Xiaoya Wang, Tao Huang, Aishui Yu*

Department of Chemistry and Shanghai Key Laboratory of Molecular Catalysis and Innovative Materials, Institute of New Energy, Fudan University, 220 Handan Road, Shanghai 200433, China

ARTICLE INFO

Article history:
Received 18 December 2008
Received in revised form 16 March 2009
Accepted 11 May 2009
Available online 20 May 2009

Keywords:
$LiFePO_4$
Hydrothermal method
Inter-site mixing
Electrochemical behavior
Lithium ion diffusion

ABSTRACT

$LiFePO_4$ has attracted broad attention as a promising cathode material for lithium ion batteries. One of the key issues related to $LiFePO_4$ performance lies on the intrinsic characteristic of Li/Fe inter-site mixing. To explore the effect of the defect chemistry on electrochemical behavior, $LiFePO_4$ is synthesized by hydrothermal method with pH value varying from 11.04 to 5.40. The results show that pure phase of $LiFePO_4$ could only be obtained at slightly basic and neutral conditions, and Rietveld refinements reveal that the degree of vacancies and inter-site mixing increase with decreasing pH value. The amounts of Fe on Li sites is nearly zero at pH value of 8.19, whereas 3.5% at 6.30. EIS measurements confirm that the occupation of Fe on Li sites will block the one-dimensional tunnel for lithium ion diffusion. It is vital to prevent the defect chemistry of $LiFePO_4$ by optimizing the synthesis conditions.

1. Introduction

Secondary lithium ion battery as an advanced energy storage system has conquered the portable electronic device market, and has great potential for HEV and EV application [1]. The development of perspective cathode material requires its natural source abundance, low cost, high safety, environment benign besides its excellent electrochemical behavior, and of particular interest, lithium iron phosphate ($LiFePO_4$) has attracted broad attention [2–5].

It is well known that the electrode reaction of $LiFePO_4$ in lithium ion battery is based on the reversible insertion/extraction of lithium ions into the chains formed by LiO_6 octahedra [6,7]. Due to its intrinsic low electronic conductivity and low lithium ion diffusion coefficient across the two-phase interface, it is essential to investigate its microstructure to have a better understanding of its defect chemistry and lithium ion migration mechanism [8,9]. Delacourt et al. found that the mixture of $xLiFePO_4$ and $(1-x)FePO_4$ could transfer to a new phase of $Li_{1-x}FePO_4$ at elevated temperature of 450 °C [10]. Yamada et al. provided direct evidence that Li_xFePO_4 could be described as a mixture of $Li_{0.05}FePO_4$ and $Li_{0.89}FePO_4$ at room temperature [1]. Focused on Li insertion/extraction in Li_xFePO_4 nanoparticles prepared by precipitation route, Gibot investigated the effect of the defect chemistry of $LiFePO_4$ on its electrochemical behavior [11].

Preparation of $LiFePO_4$ by hydrothermal method has generated considerable research activities. Lots of groups have widely studied the factors governing the particle size and morphologies of $LiFePO_4$ [12–16]. It is well known that the preparation process is crucial to the cation vacancies of $LiFePO_4$ material. In this paper, $LiFePO_4$ was prepared by hydrothermal approach, and the pH effect on the defect chemistry and inter-site mixing of the as-prepared $LiFePO_4$ was investigated as well as the importance of such defect and disorder on its electrochemical performance.

2. Experimental

2.1. Synthesis of the materials

$LiFePO_4$ was synthesized by hydrothermal route as follows: under nitrogen atmosphere, 10 mL of $FeSO_4$ solution (0.5 M), and varying amount of H_3PO_4 were transferred to a Teflon obturation vessel, then certain amount of sucrose (5% weight as that of $LiFePO_4$ to be yielded) as the reducing agent was added into the solution. After 10 mL of LiOH (1.5 M) solution was transferred into the above mentioned solution to react for about 10 min under nitrogen atmosphere, pH value of the resulting grayish white gel was measured. The pH values were controlled by the amount of LiOH or H_3PO_4 and were measured to be 11.04, 9.04, 8.19, 7.02, 6.30 and 5.40, respectively. The vessels were then sealed in a stainless steel autoclave and heated at 180 °C for 10 h. After being cooled to room temperature,

* Corresponding author. Tel.: +86 21 5566 4259; fax: +86 21 6564 2403.
E-mail address: asyu@fudan.edu.cn (A. Yu).

0378-7753/$ – see front matter © 2009 Elsevier B.V. All rights reserved.
doi:10.1016/j.jpowsour.2009.05.007

Table 1
pH values of the starting solution for all the samples and the XRD refinement factors for samples B–E.

	Sample					
	A	B	C	D	E	F
pH	11.04	9.04	8.19	7.02	6.30	5.40
Rp	–	4.56%	4.47%	4.60%	4.23%	–
Rwp	–	3.59%	3.55%	3.60%	3.27%	–

the obtained precipitates were collected by centrifugation and washed several times with deionized water and acetone. Then the samples were dried at 110 °C for 5 h in a vacuum oven and labeled as A, B, C, D, E and F, according to different pH values of 11.04, 9.04, 8.19, 7.02, 6.30 and 5.40, respectively (Table 1).

2.2. Characterization

The X-ray diffraction (XRD) measurement was carried out on a Bruker D8 Advance X-ray diffraction using Cu Kα radiation source ($\lambda = 1.5406$ Å) with a step size of 4° min^{-1} from 10° to 80°. Lattice parameters for the materials were refined by the Rietveld analysis (Accelrys MS Modeling 3.0.1). Raman spectra were recorded on Jobin Yvon. Co. LabRom-1B. The Li, Fe, P contents of the samples were analyzed by inductively coupled plasma (ICP, Thermo E.IRIS Duo) and atomic absorption spectroscopy (AAS) (Z-5000).

2.3. Electrochemical measurement

The electrochemical performance of as-prepared $LiFePO_4$ was investigated using coin cells assembled in an argon-filled glove box. The cell was composed of a lithium anode and a cathode that was a mixture of prepared $LiFePO_4$ (70%), Super P Carbon black (20%), polytetrafluoroethylene (PTFE) (10%). The mixture was rolled into a thin sheet with uniform thickness, then it was cut into 10 mm × 10 mm section before pressed to a aluminum mesh. The electrolyte was 1 M $LiPF_6$ dissolved in a mixed solvent of ethylene carbonate (EC) and dimethyl carbonate (DMC) (1:1 in weight), and Celgard 2300 was used as separator. The electrochemical impedance (EIS) measurements were performed on a CHI 660B electrochemical analysis instrument. The electrochemical charge–discharge measurements were carried out in the voltage range from 2.5 to 4.1 V vs. Li^+/Li. All the tests were performed at room temperature.

3. Results and discussion

3.1. Material identification

Fig. 1 shows the XRD patterns of all the samples. It can be clearly seen that samples B–E are single phase of $LiFePO_4$ which can be indexed to the orthorhombic olivine type structure (JCPDS no. 40-1499). Samples C–E with narrower XRD peaks indicated that they are better crystallized compared with sample B. $LiFePO_4$ cannot be obtained at strong basic condition (sample A) is due to ferrous could be more easily oxidized to ferric under strong basic condition. As for sample F which was synthesized under acidic condition, several diffraction peaks belonging to $LiFePO_4$ were obviously disappeared. The result was consistent with the previous studies that $LiFePO_4$ could only be synthesized at neutral or slightly basic pH condition by hydrothermal method [17,18].

XRD patterns of samples B–E were further analyzed by Rietveld refinements. At first, when Fe and Li occupancies are constrained to 1, the refinement results for all the four samples fit poorly with their respective XRD parameters. However, by allowing the occupancies to vary, the refinement results are greatly improved.

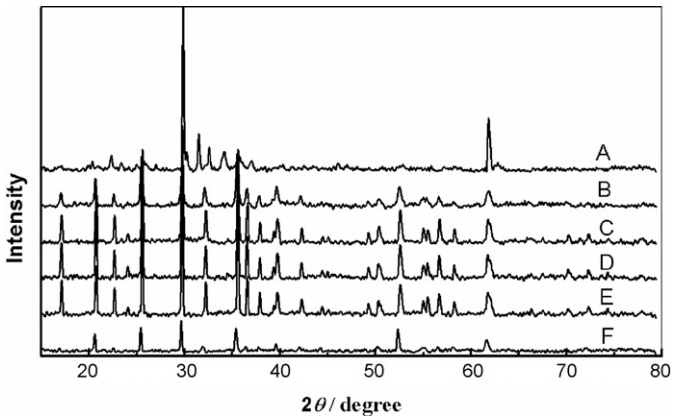

Fig. 1. XRD patterns of as-prepared $LiFePO_4$ composites which were labeled as A, B, C, D, E and F, according to different pH values 11.04, 9.04, 8.19, 7.02, 6.30 and 5.40, respectively.

According to the refinement, the formula for sample B can be described as $(Li_{0.98\square 0.02})(Fe_{0.97\square 0.03})PO_4$ with a larger cell volume of 293.69 $Å^3$, and sample C corresponds to the formula of $(Li_{0.94\square 0.06})(Fe_{0.95\square 0.05})PO_4$, with cell volumes of $V = 293.26$ $Å^3$. However, for sample D and E, good refinement results could only be done by allowing part of Fe ions on Li (4a) site, with their corresponding formulas of $(Li_{0.90}Fe_{0.02\square 0.08})(Fe_{0.92\square 0.08})PO_4$ and $(Li_{0.89}Fe_{0.035\square 0.075})(Fe_{0.90\square 0.10})PO_4$, respectively. As an example, the refinement result of sample D is depicted in Fig. 2. The refinement factors of all the samples are also given in Table 1 and the values of Rp, Rwp factors suggest the accuracy of the fittings. Therefore, according to XRD refinements results, it could be reasonable to conclude that the cation vacancies and Fe disorder are an intrinsic characteristic of $LiFePO_4$ prepared by hydrothermal method.

The Fe inter-site mixing and cell volumes as a function of pH value were presented in Fig. 3. It can be seen that with pH decreasing from 9.04 to 6.30, the degree of Fe disorder and cation vacancies in $LiFePO_4$ increased, along with the corresponding decreased cell volumes that are slightly different with the previous studies [19,20]. During hydrothermal process, at first lithium vacancies would form and then these vacancies could allow Fe to occupy under certain conditions. More vacancies could lead to more Fe on Li sites and as a result, the average Li–Li distance could be diminished with a contracted *a* and *b* axes of the lattice [10] and thus a decreased cell volume.

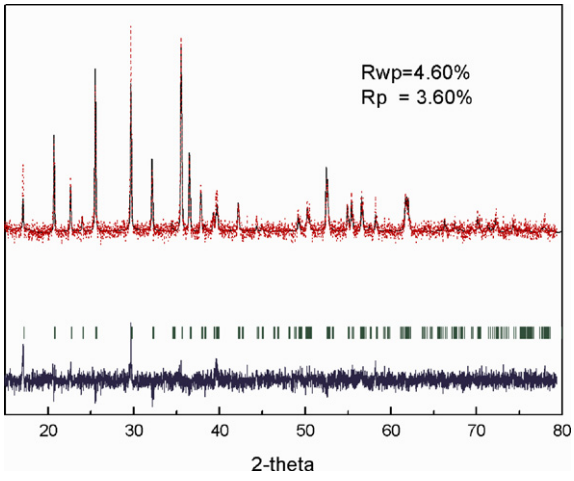

Fig. 2. Rietveld refinement of sample D.

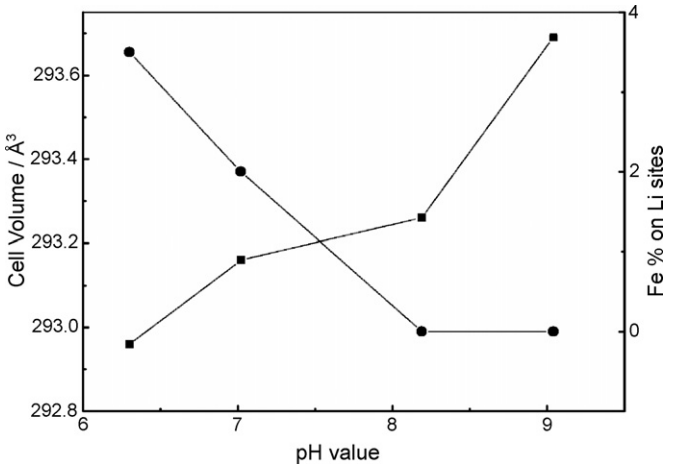

Fig. 3. Fe inter-site mixing and cell volumes as a function of pH value obtained by Rietveld refinements.

Simulation of energies for formation of intrinsic defects by Islam et al. indicated that the energies for the Li, Fe Frenkel type vacancies are about 2.15 and 5.58 eV, respectively and the energy for the Li/Fe anti-site pair is about 0.74 eV [21]. The reason for formation of cation vacancies and Fe disorder is still unknown during hydrothermal process, it could be that pH value may greatly influence the activation energy of the vacancies to be formed. With a decreased pH value, there would be more H^+ in the starting solution which has higher mobility that may affect the formation activation energy. Therefore, it may be easier to form Li vacancies and also result in Li, Fe inter-site mixing.

In order to further confirm the corresponding chemical formulas of the refinement results, the Li, Fe, P contents for samples B–E were measured. The Li/Fe and Fe/P atomic ratios determined by AAS and ICP were given in Table 2. The results suggested that non-stoichiometry issues exist in all the as-prepared products. However for samples C–E, it was basically consistent with the Rietveld refinements results. It is worth mentioning that for sample B, Fe/P atomic ratio is 1.17 which is much larger than 1. So samples B–E were conducted by Raman to further identify the impurities existing in as-prepared products. As it is shown in Fig. 4, the Raman spectrum of samples C, D, and E can be identified as the pure $LiFePO_4$ [22]. The sharp bands at 1068, 998 and 952 cm^{-1} are attributed to the intra-molecular stretching motions of PO_4^{3-}, and the weak bands between 400 and 800 cm^{-1} can be ascribed to the bending motion of PO_4^{3-}. As for sample B, the two sharp bands around 200 cm^{-1} belonging to Fe–O stretching modes of Fe_2O_3 could be observed. The reason that Fe_2O_3 of sample B cannot be detected by XRD could be that amorphous Fe_2O_3 was formed on the surface of the particle [23,24]. With Raman spectroscopy, surface characteristics rather than bulk crystalline structure could be intensified and meanwhile, the intensity of Fe–O stretching vibration at low frequency is much stronger than that of PO_4^{3-} vibration models.

Table 2
Atomic ratios of Li/Fe and Fe/P of samples B–E measured by AAS, ICP.

Sample	Li/Fe	Fe/P
B	0.71	1.13
C	1.00	1.01
D	0.98	1.01
E	0.96	1.02

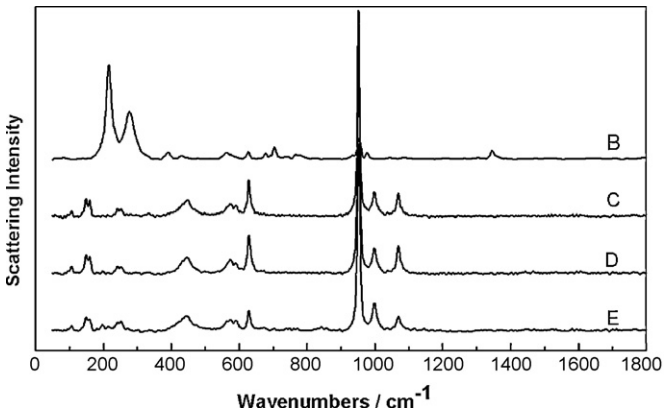

Fig. 4. Raman spectra of samples B–E.

3.2. Electrochemical performance

Fig. 5 displays the initial charge and discharge curves of the samples at the current density of 0.1 C in the potential range from 2.5 to 4.2 V. All these samples showed a good flat discharge voltage at approximately 3.4 V, which represented the typical electrochemical action of Li^+ insertion into $FePO_4$. However, sample B showed a rather poor electrochemical behavior with the initial discharge capacity of about 55 mAh g^{-1}, and this may be rooted in the inactive amorphous Fe_2O_3 formed on the surface of the sample. With the decreasing Fe inter-site mixing from E to C, the initial discharge capacity increased from 100 to 130 mAh g^{-1}.

It is well known that lithium diffusion kinetics governs the electrochemical behavior of $LiFePO_4$. Islam et al. revealed the smallest lithium migration energy along [0 1 0] one-dimensional tunnel from computational derivation [21]. Yamada et al. revealed this tunnel for lithium motion is a curved one just as shown in Fig. 7a [25]. In order to determine the influence of vacancies and inter-site Fe mixing on the lithium diffusion process for samples C–E, the subsequent electrochemical impedance (EIS) measurements were carried out in the frequency range from 10 mHz to 100 kHz at the open circuit with an ac voltage signal of 5 mV. EIS measurement for sample B was eliminated due to the impurities of Fe_2O_3 formed on the surface which is also an active material for lithium intercalation. All the Nyquist plots shown in Fig. 6a are composed of a semicircle and a line in the low frequency region. The semicircle is related to the

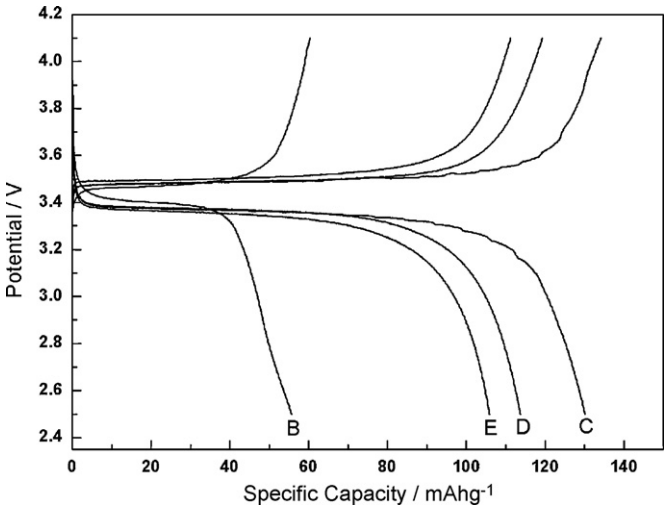

Fig. 5. Initial charge and discharge curves of samples B–E at the current density of 0.1 C in the potential range from 2.5 to 4.2 V.

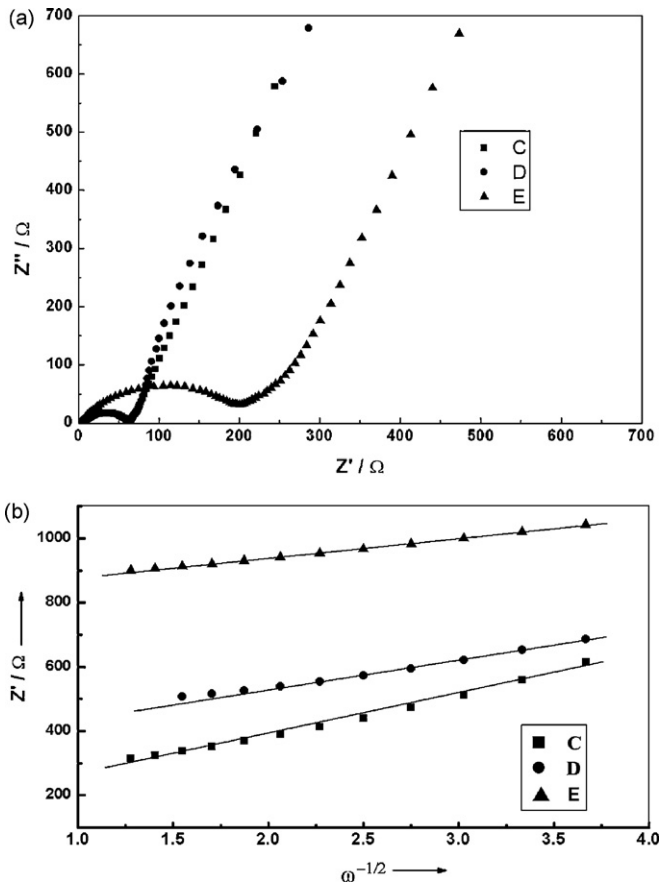

Fig. 6. (a) Electrochemical impedance spectra of samples C–E at open circuit; (b) graph of Z' plotted against $\omega^{-1/2}$.

charge transfer between the electrolyte and the active material. The straight line at the low frequency is attributed to the diffusion of lithium ions [26,27]. The lithium diffusion coefficient $\tilde{D}$ in $LiFePO_4$ electrode could be calculated by Eq. (1):

$$D = \frac{R^2T^2}{2A^2n^4F^4C^2\sigma^2} \quad (1)$$

where R is the gas constant, T is the room absolute temperature in our experiment, A is the surface area of the electrode, n is the number of electrons per molecule attending the electronic transfer reaction, F is Faraday constant, C is the concentration of lithium ion in $LiFePO_4$ electrode, respectively. The plots of Z_{re} against $\omega^{-1/2}$ were depicted in Fig. 6b, it corresponding to Eq. (2), and σ is the slope of the straight line.

$$Z'' = \sigma\omega^{-1/2} \quad (2)$$

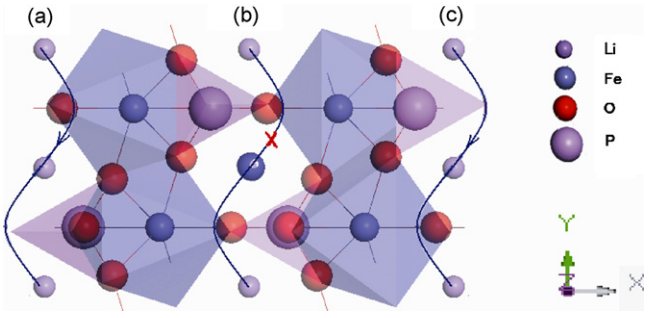

Fig. 7. (a) Curved pathway for lithium ion motion along [0 1 0] direction; (b) the blocked tunnel by absence of Fe on Li sites.

The lithium diffusion coefficients $\tilde{D}(cm^2\,S^{-1})$ of samples C, D, E calculated by the equation were 2.56×10^{-13}, 1.19×10^{-13}, 5.83×10^{-14}, respectively. It is clear that the lithium ion diffusion coefficient decreases with increasing of cation vacancies and inter-site Fe mixing. It suggests that the occupation of Fe on Li sites would block the one-dimensional pathway of lithium as shown in Fig. 7b. Since during the process of lithium migration, the lithium vacancies would continue to migrate in the opposite direction [28], the lower anti-site cation mobility would prohibit lithium vacancies migrating along [0 1 0] tunnels. The larger amount of Fe on Li sites for the product, the lower lithium ion diffusion coefficients it has, and therefore, the defect chemistry of $LiFePO_4$ will greatly affect lithium insertion/extraction behavior.

4. Conclusions

$LiFePO_4$ was successfully prepared at neutral and slightly basic pH conditions by hydrothermal method. XRD and Rietveld refinements suggest that with decrease of pH value, the degree of Fe inter-site mixing and cation vacancies increases which was further confirmed by element analyses. The occupation of Fe on Li sites will block the curved one-dimensional tunnel for lithium motion. The diffusion coefficient measurements showed that with lower cation vacancies and lower Fe mixing degree, samples C give D value of $2.56 \times 10^{-13}\ cm^2\,S^{-1}$, whereas decreased to $5.83 \times 10^{-14}\ cm^2\,S^{-1}$ with increasing of cation vacancy and Fe mixing. By optimizing the synthesis conditions to minimize the defect chemistry of $LiFePO_4$, hydrothermal method would have great potential for low cost, large scale $LiFePO_4$ production.

Acknowledgement

This work is financially supported by Science & Technology Commission of Shanghai Municipality (08DZ2270500), China.

References

[1] A. Yamada, H. Koizumi, S.-I. Nishimura, N. Sonoyama, R. Kanno, M. Yonemura, T. Nakamura, Y. Kobayashi, Nat. Mater. 5 (2006) 357–360.
[2] B.L. Ellis, W.R.M. Makahnouk, Y. Makimura, K. Toghill, L.F. Nazar, Nat. Mater. 7 (2008) 665–671.
[3] Y.G. Wang, Y.R. Wang, E. Hosono, K.X. Wang, H.S. Zhou, Angew. Chem. Int. Ed. 47 (2008) 1–6.
[4] A.K. Padhi, K.S. Nanjundaswamy, C. Masquelier, J.B. Goodenough, J. Electrochem. Soc. 144 (1997) 1609–1613.
[5] M. Yonemura, A. Yamada, Y. Takei, N. Sonoyama, R. Kanno, J. Electrochem. Soc. 151 (2004) A1352–A1356.
[6] M.S. Whittingham, Chem. Rev. 104 (2004) 4271–4301.
[7] A.K. Padhi, K.S. Nanjundaswamy, J.B. Goodenough, J. Electrochem. Soc. 144 (1997) 1188–1194.
[8] S.Y. Chung, J.T. Bloking, Y.M. Chiang, Nat. Mater. 1 (2002) 123–128.
[9] P.S. Herle, B. Ellis, N. Coombs, L. Nazar, Nat. Mater. 3 (2004) 147–152.
[10] C. Delacourt, P. Poizot, J.-M. Tarascon, C. Masquelier, Nat. Mater. 4 (2005) 254–260.
[11] P. Gibot, M.C. Cabanas, L. Laffonont, S. Levasseur, P. Caralach, S. Hamelet, J.-M. Tarascon, C. Masquelier, Nat. Mater. 7 (2008) 741–747.
[12] S.F. Yang, P.Y. Zavalij, M.S. Whittingham, Electrochem. Commun. 3 (2001) 505–508.
[13] S. Tajimi, Y. Ikeda, K. Uematsu, K. Toda, M. Sato, Solid-State Ionics 175 (2004) 287–290.
[14] K. Kanamura, S. Koizumi, K. Dokko, J. Mater. Sci. 43 (2008) 2138–2142.
[15] J.J. Chen, M.J. Vacchio, S.J. Wang, N. Chernova, P.Y. Zavalij, M.S. Whittingham, Solid-State Ionics 178 (2008) 1676–1693.
[16] K. Dokko, S. Koizumi, K. Sharaishi, K. Kanamura, J. Power Sources 165 (2007) 656–659.
[17] J. Lee, A.S. Teja, J. Supercrit. Fluids 35 (2005) 83–90.
[18] K. Dokko, S. Koizumi, K. Kanamura, Chem. Lett. 35 (2006) 338–339.
[19] J.J. Chen, M.S. Whittingham, Electrochem. Commun. 8 (2006) 855–858.
[20] Z.L. Wang, S.R. Su, C.Y. Yu, Y. Chen, D.G. Xia, J. Power Sources 184 (2008) 633–636.
[21] M.S. Islam, D.-J. Driscoll, C-A.J. Fisher, P.-R. Slater, Chem. Mater. 17 (2005) 5085–5092.
[22] C.M. Burba, R. Frech, J. Electrochem. Soc. 151 (2004) A1032–A1038.

[23] K. Dokko, K. Shiraishi, K. Kanamura, J. Electrochem Soc. 152 (2005) A2199–A2202.
[24] K. Shiraishi, K. Dokko, K. Kanamura, J. Power Sources 146 (2005) 555–558.
[25] S.I. Nishimura, G. Kobayashi, K. Ohoyama, R. Kanno, M. Yashima, A. Yamada, Nat. Mater. 7 (2008) 701–711.
[26] F. Gao, Z.Y. Tang, Electrochim. Acta 53 (2008) 5071–5075.
[27] X.Z. Liao, Z.F. Ma, Q. Gong, Y.S. He, L. Pei, L.J. Zeng, Electrochem. Commun. 10 (2008) 691–694.
[28] C.A.J. Fisher, V.M.H. Prieto, M.S. Islam, Chem. Mater. 20 (2008) 5907–5915.